COBEM 2021 26th International Congress of Mechanical Engineering
ABCM Associação Brasileira de Engenharia e Ciências Mecânicas
November 22-26, 2021, Virtual Congress, Brazil

COB-2021-0765
NUMERICAL NONLINEAR DYNAMICS STUDY OF A SIMPLIFIED TWO-PHASE FLOW MODEL FOR PIPELINE-RISER SYSTEMS

Adilson Paulo de Miranda Junior
Karl Peter Burr
Universidade Federal do ABC

miranda.adilson@ufabc.edu.br, karl.burr@ufabc.edu.br

Abstract. *Nonlinear dynamics of multi-phase flow in pipeline-riser systems is studied as a function of the system parameters and boundary conditions. The pipeline and the riser are both modeled as control volumes. For the pipeline, liquid and mass conservation equations are considered and the flow regime is assumed as always stratified. The pipeline void fraction follows from the local balance among gas and liquid wall friction forces, gas-liquid interfacial friction force and gravity force. For the riser, liquid and gas mass conservation and linear momentum balance equations are considered plus a kinematic relation to close the model. The resulting model is composed of three differential equations and a set of algebraic equations, and therefore, contains the minimum conditions to present chaotic behavior. It is also simple enough to allow a numerical study of its nonlinear dynamics with techniques, such as Poincare maps and the evaluation of Lyapunov exponents. These techniques are used to numerically map the regions in the system parameters and boundary conditions space with stable and unstable stationary states, with periodic orbits and possibly with chaotic behavior.*

Keywords: *Two-phase Flow, Pipeline-riser system, Numerical Simulation, Nonlinear dynamics, Poincare Maps*

1. INTRODUCTION

Offshore oil production system may observe intermittent behavior along its life span with the reduction of oil and gas mass flow rate coming from the oil fields. This is a terrain induced phenomenon. Whenever a sub-sea pipline has a downward section followed by an upward section, like a vertical riser connected to the the platform, liquid may accumulate at the riser base and partially or totally block gas passage from the pipeline to the riser.

For partial gas blockage, an oscillatory flow regime arises which is apparently periodic. On the other hand, when gas blockage occurs, it continues until the gas pressure in the pipeline is large enough to push the liquid slug out of the pipeline and to start gas penetration into the riser. At this point different scenarios are possible. If the liquid slug pushed by the gas did not fill in the whole riser, gas bubbles penetrate into the riser, decreasing the pressure along the riser and making the gas-liquid mixture to flow to the separator. The gas pressure in the pipeline decreases until the gas passage at the base of the riser is blocked again by the liquid and the cycle starts again. This periodic behavior is coined periodic orbit or limit cycle in terms of the system dynamics point of view. If the liquid slug pushed by the gas has already filled in the whole riser, the separator has been seeing only liquid by the time the gas is able to push the liquid slug out of the pipeline. The gas pressure at the pipeline reached its maximum when bubble penetration into the riser had started. This stage is characterized by a rapidly expanding gas bubble that continuously overruns the liquid in the riser and leaves a thin liquid film along the riser wall. During this stage, the separator sees a gas burst and the gas inventory in the pipeline decreases steadily with a corresponding rapid decrease in the pipeline pressure. At some point, the gas velocity in the riser becomes insufficient to support a cocurrent liquid film along the riser wall and the liquid starts to fall back to the riser bottom (countercurrent flow). As a result, liquid starts to accumulate at the riser bottom, the gas passage is blocked, and the cycle starts again. The last intermittent regime described above is known as severe slugging phenomenon in the literature.

The first work using a system dynamics approach to model the intermittent flow regimes described above is Zakarian and Tran (1999). A control volume approach was used to model the two-phase flow in pipeline-riser systems, which consists of a system of algebraic-differential equations (DAE) with only two differential equations. This model has a single stationary point which loses statility in the system parameter space through a supercritical Hopf bifurcation given rise to a stable limit cycle. Normal form theory is applied to the model equations to obtain an aproximate solution for the limit cycle. Since this model has only one degree of freedom, its dynamics has limit sets restricted to fixed points and limit cicles.

Baliño *et al.* (2010) modeled two-phase flows in pipeline-riser systems with risers in catenary form. The riser was modeled as a distributed system, but the pipeline was modeled as a control volume. Stability map for the single stationary state in the system parameter space was built by numerical integration in time of the system governing equations with the stationary state as the initial condition.

Azevedo *et al.* (2015) and Azevedo *et al.* (2017) used linear stability analysis to construct stability maps for the single stationary state in the system parameter space. Azevedo *et al.* (2015) studied the effect of different severe slugging mitigation mechanisms on the stationary state stability and Azevedo *et al.* (2017) studied the effect of the pipeline modeling in the stationary state stability.

Burr and Baliño (2015) presented an asymptotic theory to obtain an evolution equation for the system instability. This evolution equation has a limit cycle solution which approximate the limit cycle of the original system, and then allows to obtain estimates for the limit cycle period and the evolution of quantites of interest along the limit cycle, such as riser bottom pressure, for example. This theory is valid for parameters close to the Hopf bifurcation surface in the system parameter space.

The literature listed above addresses only aspect of the dynamics of two-phase flows in pipeline-riser systems, like linear and nonlinear stability analysis and approximate theories to capture the limit cycle related to the supercritical Hopf bifurcation observed for the various models for two-phase flows in pipleine-riser systems. No previous work presents a thorough study of the dynamics of two-phase flow in pipeline-riser system, which is the objctive of the present work. A simplified pipeline-riser system two-phase flow model consisting of a DAE system with three differential equations is considered. This model is simple enough to allow numerical study of its nonlinear dynamics with techniques such as the Lyapunov function, Poincaré maps and evaluation of Lyapunov exponents, and it contains the minimum condition to display chaotic behavior.

The next section presents the pipeline-riser system two-phase flow model considered in this work. The methodology to study numerically the nonlinear dynamics of the considered model is described in the third section. Results from the numerical study of the model nonlinear dynamics are given in the fourth section. A discussion of the results, conclusions and future work are given in the fifth section.

2. PIPELINE-RISER TWO-PHSE FLOW MODEL

The pipeline-riser system is composed by a straigh pipeline plus a gas buffer and a riser. The pipeline has length L_p and inclination angle β with respec to the horizontal. The riser is a straight pipe with length L_r and has inclination angle θ with respect to the horizontal. The gas buffer has volume V_b. The pressure at the riser top is the separator presure P_s. Gas enters the pipeline-riser system through the gas buffer with mass flow rate M_{g0} and the liquid enters at the begining of the pipeline with volumetric flow rate Q_{l0}, as illustrated in Fig. 1 below.

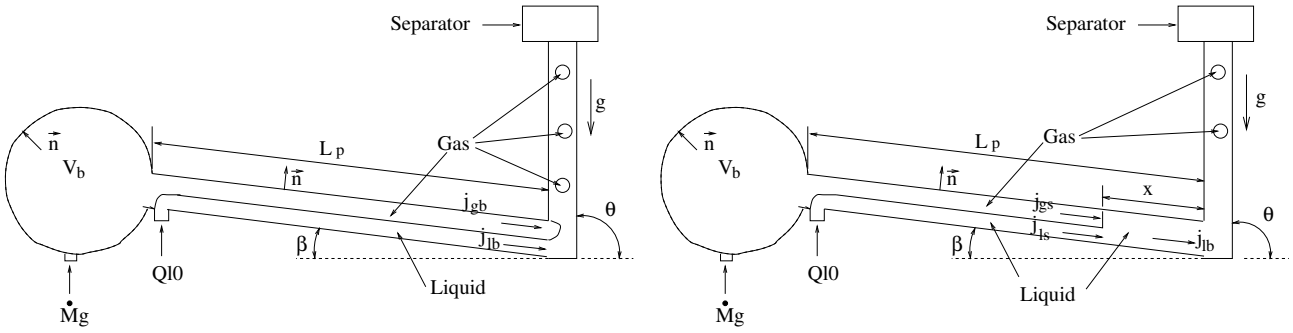

(a) First Configuration, part (A)

(b) Second Configuration, part (B)

Figure 1. Pipeline riser system with continuous gas passage from the pipeline to the riser (first configuration, part (A)) and with partial pipeline flooding with liquid (second configuration, part (B))

The gas-liquid flow in the pipeline is assumed as always stratified, which extends to the whole pipeline or up to the liquid front flooding the pipeline. The flooded section of the pipeline has length x as illustrated in part (B) of Fig. 1. The gas pressure at the stratified section of the pipeline is assumed uniform. Two configurations are considered for the pipeline. The first configuration ($x = 0$) corresponds to continuous gas flow from the pipeline into the riser and the second configuration ($x > 0$) corresponds to no gas flow from the pipeline into the riser and partial pipeline flooding with liquid.

The pipeline plus buffer is modeled as a control volume. Liquid and mass conservation equations are considered and the pipeline void fraction α_p follows from a local balance among liquid and gas wall friction forces, the gas-liquid interfacial force and the gas-liquid gravitational force component along the tube axis under the assuption of fully developed flow regime. This approach results in a DAE system as governing equations for the pipeline two-phase flow for both configurations.

The two-phase flow in the riser is modeled by an isothermal one-dimensional drift-flux model, where mass conservation for each phase and a linear momentum equation without the inertial terms for the mixture are considered plus a closure relation, which is a kinematic relation that fixes the relative velocity between phases. The liquid and gas conservation equations and the linear momentum equation are integrated in space along the riser length, resulting in a DAE system with respect to the flow variables at the bottom and top of the riser. The kinematic relation is imposed at riser top and bottom, resulting in two more algebraic equations.

The two-phase flow governing equations are given in terms of non-dimensional variables. The adotped scales and the relation between dimensional and non-dimensional form of the variables is given by the equation

$$\tilde{t} = t\frac{Q_{l0}}{AL_r},\ \tilde{j} = j\frac{A}{Q_{l0}},\ \tilde{P} = \frac{P}{\rho_l R_g T},\ \tilde{x} = \frac{x}{L_r},\ \tilde{\dot{M}}_{g0} = \frac{\dot{M}_{g0}}{\rho_l Q_{l0}}, \tag{1}$$

where t stands for time, A is the pipe cross-sectional area, j stands for superficial velocity, P stands for pressure, ρ_l is the liquid density, $\tilde{\dot{M}}_{g0}$ is the ratio between the gas mass flow rate and the liquid mass flow rate, and R_g and T_g are, respectively, the gas constant and temperature. The variables with a $\tilde{}$ are non-dimensional, but in what follows the tilde is omitted to simplify the notation, but all variables are non-dimensional.

2.1 Governing Equations for Configuration $x = 0$

For the configuration with continuous gas passage from the pipeline into the riser bottom, the pipeline-riser two-phase flow is governed by the following set of equations:

$$\frac{dm_l}{dt} = j_{l,b} - j_{l,t} = h_1, \tag{2}$$

$$\frac{1}{2}\alpha_b\frac{dP_b}{dt} = P_b j_{g,b} - P_t j_{g,t} + \frac{P_t + P_b}{2}\left(j_{l,b} - j_{l,t}\right) = h_2, \tag{3}$$

$$\frac{L_p}{L_r}\frac{d\alpha_p}{dt} = j_{l,b} - 1 = h_3, \tag{4}$$

$$h_4 = \frac{\alpha_b}{2}\left[\tilde{\dot{M}}_{g0} - \tilde{P}_b\left(j_{g,b} + j_{l,b} - 1\right)\right] - \tilde{\alpha}_p\left[P_b j_{g,b} - P_t j_{g,t} + \frac{P_t + P_b}{2}\left(j_{l,b} - j_{l,t}\right)\right] = 0, \tag{5}$$

$$\begin{aligned} h_5 =& P_t - P_b + \frac{1}{2}\left\{\left[(1-\alpha_t) + P_t\alpha_t\right]\left(\pi_G \sin\theta_t + 2\pi_F f_m(Re, m_t; \epsilon/D) j_t|j_t|\right)\right. \\ &\left. + \left[(1-\alpha_b) + P_b\alpha_b\right]\left(\pi_G \sin\theta_b + 2\pi_F f_m(Re, m_b; \epsilon/D) j_b|j_b|\right)\right\} = 0, \end{aligned} \tag{6}$$

$$h_6 = j_{g,b} - \alpha_b(C_{d,b} j_b + U_{d,b}) = 0, \tag{7}$$

$$h_7 = j_{g,t} - \alpha_t(C_{d,t} j_t + U_{d,t}) = 0, \tag{8}$$

$$h_8 = A_p\left(\frac{1}{2}(1 + j_{l,b}), \frac{1}{2}\left(j_{g,b} + \frac{\tilde{\dot{M}}_{g0}}{P_b}\right), p_b, \alpha_p\right) = 0, \tag{9}$$

$$h_9 = m_l - \frac{1}{2}\left(2 - \alpha_b - \alpha_t\right) = 0, \tag{10}$$

$$h_{10} = x = 0, \tag{11}$$

$$h_{11} = j_{g,s} - j_{g,b} = 0, \tag{12}$$

$$h_{12} = j_{l,s} - j_{l,b} = 0, \tag{13}$$

where the subscript b (t) represents quantites at the riser bottom (top). Then, $j_{l,b}, j_{g,b}, P_b, \alpha_b$ ($j_{l,t}, j_{g,t}, P_t, \alpha_t$) are respectively, the liquid superficial velocity, the gas superficial velocity, the pressure and the void fraction at the riser bottom (top). m_l represents the mass of liquid in the riser. α_p represents the pipeline stratified region void fraction and $\bar{\alpha}_p = V_b/(AL_r) + (L_p/L_r)\alpha_p$. $\pi_G = gL_r/(R_g t_g)$ and $\pi_F = (L_r/D)(Q_{l0}/A)^2/(R_g T_g)$ are non-dimensional numbers. $R_{e,m}$ is the mixture Reynolds number given by the equation

$$R_{e,m} = \frac{\rho_l D Q_{l0}}{A\mu_l} \frac{(1-\alpha+P\alpha)|j|}{1-\alpha+\delta_\mu \alpha} \tag{14}$$

where μ_l is the liquid dynamic viscosity, j is the total superficial velocity and δ_μ is the ratio between the gas and liquid dynamic viscosities. f_m is the Fanning friction factor for the mixture, given in Chen (1979) and function of the mixture Reynolds number and of the non-dimensional pipe wall roughness ϵ/D. The distribution parameter CD and the void-weighted mean drift velocity UD appearing in Eq. (7) and (8) are given by Bendiksen correlation (see Bendiksen (1984)).

Equation (2) is the liquid mass conservation equation integrated along the riser lenght. Eq. (3) is the gas mass conservation equation minus the pressure times the liquid mass conservation equation integrated along the riser lenght. Eq. (4) is the liquid mass conservation for the pipeline. The integral along the riser lenght of the linear momentum equation results in Eq. (6). Eqs. (7) and (8) are the kinematic relation specifying the relative velocity between phases for the riser applied at the riser bottom and top, respectively. The algebraic Eq. (5) results from the gas mass conservation equation for the pipeline and from Eq. (3) after eliminating the riser bottom pressure time derivative appearing in both equations. In Eq. (9), the form of the function $A_p(j_l, j_g, P, \alpha_p)$ is given by

$$A(j_l, j_g, P, \alpha_p) = P f_i (\frac{j_g}{\alpha_p} - u_i)|\frac{j_g}{\alpha_p} - u_i| \frac{\gamma_i}{\alpha_p(1-\alpha_p)} - f_l j_l |j_l| \frac{\gamma}{(1-\alpha_p)^3} + P f_g j_g |j_g| \frac{(1-\gamma)}{\alpha_p^3} + \frac{1}{2}\pi_D (1-P)\sin\beta \tag{15}$$

where u_i is the liquid-gas interface velocity, P is the gas pressure, j_l is the liquid superficial velocity and j_g is the gas superficial velocity. f_i, f_l, f_g are, respectively, the liquid-gas interface friction factor and the liquid and gas wall friction factors. $\gamma(\gamma_i)$ is angle corresponding to the liquid wetted (interface) perimeter. $\pi_D = gDQ_{l0}^2/A^2$ is a non-dimensional number. Eq. (15) is obtained form the one-dimensional two-fluid model for stratified flow by subtracting the gas linear momentum equation from the liquid linear momentum equation under the hypothesis of fully developed flow. This results in the balance among the gas and liquid wall friction forces, the gas-liquid interface friction force and the gravitational force component in the tube axis direction.

Eq. (10) is the liquid mass in the riser written in terms of the void fraction at the top and bottom of the riser. Eqs. (11)-(13) exists since these quantities are non zero for the second configuration ($x > 0$), where the zero quantities will be $j_{g,b}$ and α_b. The superficial velocities $j_{l,s}$ and $j_{g,s}$ are, respectively, the liquid and gas superficial velocities at the liquid flooding front in the second configuration ($x > 0$).

2.2 Governing Equations for configuration $x > 0$

The configuration with partial pipeline flooding with liquid is governed by equations similar to the set of equations given for the first configuration. Here, only the equations that has changed are displayed. These equations are:

$$\left(\frac{L_b}{L_e} + \alpha_p\left(\frac{L_p}{L_r} - x\right)\right)\left\{\frac{dP_b}{dt} - \pi_G \sin\beta \frac{dx}{dt}\right\} = \tilde{M}_{g0} - (P_b - \pi_G x \sin\beta)(j_{l,b} - 1 + j_{g,s}) = h_2 \tag{16}$$

$$\alpha_p \frac{dx}{dt} = -j_{g,s} = h_3 \tag{17}$$

$$\left(\frac{L_p}{L_r} - x\right)\frac{d\alpha_p}{dt} = j_{l,b} - 1 - j_{g,s} = h_4 \tag{18}$$

$$h_5 = P_t - P_b + \frac{1}{2}\left\{[(1-\alpha_t) + P_t\alpha_t]\left(\pi_G \sin\theta_t + 2\pi_F f_m(Re, m_t; \epsilon/D) j_t |j_t|\right)\right. \\ \left. + \pi_G \sin\theta_b + 2\pi_F f_m(Re, m_b; \epsilon/D) j_{l,b}|j_{l,b}|\right\} = 0, \tag{19}$$

$$h_6 = P_t j_{g,t} + \frac{P_t + P_b}{2}(j_{l,t} - j_{l,b}) = 0 \tag{20}$$

$$h_7 = j_{g,t} - \alpha_t \left(C_{d,t}(j_{l,t}, j_{g,t}, P_t, \alpha_t) j_t + U_{d,t}(j_{l,t}, j_{g,t}, P_t, \alpha_t)\right) = 0, \tag{21}$$

$$h_8 = A_p\left(\frac{1}{2}(1 + j_{l,s}), \frac{1}{2}\left(j_{g,s} + \frac{\tilde{M}_{g0}}{P_b - \pi_G x \sin\beta}\right), P_b - \pi_G x \sin\beta, \alpha_p\right) = 0, \tag{22}$$

$$h_9 = m_l - 1 + \frac{\alpha_t}{2} = 0, \tag{23}$$

$$h_{10} = j_{g,s} - \alpha_p(j_{l,b} - j_{l,s}) = 0, \tag{24}$$

$$h_{11} = j_{g,b} = 0, \tag{25}$$

$$h_{12} = \alpha_b = 0. \tag{26}$$

Equations (16) and (18) results, respectively, from the pipeline gas and liquid mass conservation equations for this configuration and the kinematic condition at the liquid penetration front. Eq. (17) follows from kinematic condition at the liquid penetration front. Eq. (20) results from the gas mass conservation equation integrated along the riser lenght minus the riser top pressure multiplying the integral of the liquid mass conservation along the riser lenght with $j_{g,b} = \alpha_b = 0$. Eq. (21) is the kinematic relation specifying the relative velocity between phases at the riser top. For cocurrent flow CD and UD are given by Bendiksen correlation, but if countercurrent flow happens, then CD and UD are given by Chexal *et al.* (1997) correlation. In Eq. (22), $A_p(j_l, j_g, P, \alpha_p)$ is given by Eq. (15) but with different expressions for j_l, j_g and P. Eq. (23) has the same meaning as Eq. (9), but now $\alpha_b = 0$. Eq. (24) follows form the liquid mass conservation for the pipeline, from the liquid mass conservation for the stratified part of the pipeline only and from Eq. (17). Eqs. (25) and (26) representes, respectively, the fact that now $j_{g,b} = \alpha_b = 0$.

2.3 Swithching Conditions Between Configurations

For numerical time integration of the model governing equations it is necessary to specify the transition form the first model configurarion ($x = 0$) equations to the second model configuration ($x > 0$) equations and the other way around. For example, for a given set of initial conditions the numerical time integration starts with the governing equations for the first configuration ($x = 0$), and assume that as $t \to t_0^-$, $\alpha_b \to 0$ and $j_{gb} \to 0$. This implies that at $t = t_0$ the equations for the first configuration are not valid anymore, but the numerical time integration can be continued if the governing equations for the second configuration ($x > 0$) are used and if appropriate initial conditions for them are given. These are the transition conditions. At the transition most variables are continuous. Discontinuities may appear at the transition for riser base superficial velocities and void fraction.

Assume t_0 to be an instant to switch from one configuration to the other. To make the transition from the second configuration ($x > 0$) to the first configuration ($x = 0$) at the instant t_0, the superficial velocities at instant t_0^+ (configuration $x > 0$) can be determined as follows:

$$j_{g,s}^+ = j_{g,b}^+, \;\; j_{l,s}^+ = j_{l,b}^+, \;\; j_{g,b}^+ = -\alpha_p \frac{dx^-}{dt}, \;\; j_{l,b}^+ = j_{l,b}^- + \alpha_p \frac{dx^-}{dt} \tag{27}$$

and α_b^+ is given by Eq. (7). To make the transition from the first configuration ($x = 0$) to the second configuration ($x > 0$) at the instant t_0, it can be shown that the superficial velocities at instant t_0^+ (configuration $x = 0$) can be determined as follows:

$$j_{g,b}^+ = j_{g,s}^+ = j_{g,b}^- = 0, \;\; j_{l,s}^+ = j_{l,b}^+ = j_{l,b}^-. \tag{28}$$

2.4 Governing Equations in Matrix Form

The DAE system for both configurations can be written in matrix form

$$\mathbf{M}\left(\mathbf{z}\right)\frac{\partial}{\partial t}\mathbf{z}=\mathbf{h}\left(\mathbf{z},\boldsymbol{\lambda}\right) \tag{29}$$

where $\mathbf{z}^T=\{j_{l,b}\ j_{l,t}\ j_{g,b}\ j_{g,t}\ P_b\ \alpha_b\ \alpha_t\ \alpha_p\ m_l\ x\ j_{g,s}\ j_{l,s}\}$. The lines of vector $\mathbf{h}$ for the first (second) configuration are given by Eqs. (2)-(13) (Eqs. (2) and (16)-(26)). $\boldsymbol{\lambda}$ represents the set of system parameters and boundary conditions. The non-zero elements of the matrix $\mathbf{M}(\mathbf{z})$ for the first configuration are $\mathbf{M}_{1,9}=1,\ \mathbf{M}_{2,5}=\frac{\alpha_b}{2},\ \mathbf{M}_{3,8}=L_p/L_r$, and for the second configuration they are $\mathbf{M}_{1,9}=1,\ \mathbf{M}_{2,5}=(L_p/L_r+\alpha_p(L_p/L_r-x)),\ \mathbf{M}_{2,10}=-\pi_G\sin\beta(L_p/L_r+\alpha_p(L_p/L_r-x)),\mathbf{M}_{3,10}=\alpha_p,\ \mathbf{M}_{4,8}=(L_p/L_r-x)$. The DAE system given by Eq. (29) can be written in semi-explicit form

$$\begin{array}{rl}\dot{\mathbf{x}} & =\mathbf{f}(\mathbf{x},\mathbf{y},\boldsymbol{\lambda})\\ 0 & =\mathbf{g}(\mathbf{x},\mathbf{y},\boldsymbol{\lambda})\end{array} \tag{30}$$

with $\mathbf{x}^T=\{P_b\ \alpha_p\ m_l\}$, $\mathbf{y}^T=\{j_{l,b}\ j_{l,t}\ j_{g,b}\ j_{g,t}\ \alpha_b\ \alpha_t\ x\ j_{g,s}\ j_{l,s}\}$ and $\mathbf{g}^T=\{h_4\ h_5\ h_6\ h_7\ h_8\ h_9\ h_{10}\ h_{11}\ h_{12}\}$ for the first configuration, but with $\mathbf{x}^T=\{P_b\ \alpha_p\ x\ m_l\}$, $\mathbf{y}^T=\{j_{l,b}\ j_{l,t}\ j_{g,b}\ j_{g,t}\ \alpha_b\ \alpha_t\ j_{g,s}\ j_{l,s}\}$ and $\mathbf{g}^T=\{h_5\ h_6\ h_7\ h_8\ h_9\ h_{10}\ h_{11}\ h_{12}\}$ for the second configuration.

3. NONLINEAR DYNAMICS STUDY

Most of the dependent variables in the DAE system given by Eq. (29) or by Eq. (30) (semi-explicit form) can assume values in a fixed domain. The void fractions α_b,α_t and α_p assume values in the interval $[0,1]$ only. The pressure at the riser top P_t is a parameter and is equal to the separator presure P_s. The pressure at the riser bottom assume values in the interval $[P_t,P_t+\pi_G]$, since the maximum pressure at the riser bottom occurs when it is totally filled with liquid. The gas superficial velocities $j_{g,b}$ and $j_{g,t}$ are always positive, but has in principle no definite upper limit. The liquid superficial velocity $j_{l,b}$ is always positive, but it has no definite upper bound. The superficial velocity $j_{l,t}$ is usually positive, but it may assume negative values for the second configuration when severe slugging occurs. The riser liquid mass m_l assume values in the interval $[0,1]$. The pipeline flooding length x always assume zero or positive values. This discussion gives an ideia of the range of values the dependent variables can assume.

The trajectories of the DAE system given by Eq. (29) or by Eq. (30) are constrained to the set $\mathbb{L}$ defined as

$$\mathbb{L}=\{(\mathbf{x},\mathbf{y})\in\mathbb{X}\times\mathbb{Y}:\mathbf{g}(\mathbf{x},\mathbf{y},\boldsymbol{\lambda})=0\} \tag{31}$$

where $\mathbf{x}\in\mathbb{X}\subset\mathbb{R}^n,\mathbf{y}\in\mathbb{Y}\subset\mathbb{R}^m,\boldsymbol{\lambda}\in\mathbb{P}\subset\mathbb{R}^q$. For the first configuration, $n=3$ and $m=9$ and for the second configuration $n=4$ and $m=8$. The trajectories of the DAE system given by Eq. (29) or by Eq. (30) are in the set

$$\mathbb{M}=\{(\mathbf{x},\mathbf{y})\in\mathbb{L}:\text{rank}(D_{\mathbf{x}}\mathbf{g})=n\text{ and rank}(D_{\mathbf{y}}\mathbf{g})=m\} \tag{32}$$

with n and m given in the previous paragraph according to the configuration. $\mathbb{M}$ is a regular subset of $\mathbb{L}$, which by the Implicit Function Theorem (IFT), is an n-dimensional manifold. The set

$$\mathbb{S}=\{(\mathbf{x},\mathbf{y})\in\mathbb{L}:\Delta(\mathbf{x},\mathbf{y}):=\det D_{\mathbf{y}}\mathbf{g}=0\} \tag{33}$$

is called the singular surface or the singularity. Typically no solution exists for points in $\mathbb{S}$. A thorough discussion on the effects of singularyties in DAE system dynamics is given in Venkatasubramanian *et al.* (1995). For points $(\mathbf{x},\mathbf{y})\in\mathbb{M}$, the IFT garantees that there is a function $\mathbf{y}$ such that $\mathbf{g}(\mathbf{x},\mathbf{u})=0$ if and only if $\mathbf{u}=\mathbf{y}(\mathbf{x})$. Then the study of the DAE system has been reduced to the study of

$$\dot{\mathbf{x}}=\mathbf{f}(\mathbf{x},\mathbf{y}(\mathbf{x})). \tag{34}$$

Therefore, on the manifold $\mathbb{M}$ the dynamics of the DAE system given by Eq. (29) or Eq. (30) reduces to the dynamics of the ordinary differential equation (ODE) represented by the Eq. (34). Then, results for linear stability and bifurcation from ODEs can be applied to the considered DAE system.

For the first configuration, the set $\mathbb{S}$ is related to $j_{g,b} = \alpha_b = 0$, since in this case it is easy to see that $D_{\mathbf{y}}\mathbf{g} = 0$. Just as this situation occurs there is the switch to the second configuration where $D_{\mathbf{y}}\mathbf{g} \neq 0$. Besides the situation described above, it is assumed that $D_{\mathbf{y}}\mathbf{g} \neq 0$ for the first configuration restricted to the domain described at the beginning of this section. Regarding the second configuration, unless the pipeline is totally flooded, the same assumption $D_{\mathbf{y}}\mathbf{g} \neq 0$ seems correct. Therefore, the manifold $\mathbb{M}$ is basically the entire domain of allowable values for the dependent variables in both configurations and the DAE system dynamics should be given by the dynamics of the reduced ODE, given by Eq. (34). Another consequence is that the DAE system has differential index one (see Brenan *et al.* (1995) and Beardmore and Song (1998)).

Next, the stationary points evaluation and their statibility are discussed. Then the nonlinear stability of the stationary points are addressed by constructing a Lyapunov function, which allow to obtain estimates for the stationary points basin of attraction. Poincaré map is proposed to search numerically for periodic orbits and to study their stability. Poincaré map is also used to investigate the possibility of chaotic behavior, which can be associated with orbit divergence for very close initial conditions. Numerical evaluation of the Lyapunov exponents for specific orbits is used to investigate orbit divergence and therefore the possibility of chaotic behavior.

3.1 Stationary Points and Linear Stability

There is only one stationary state for the first configuration ($x = 0$), which can be computed by solving the equation

$$\mathbf{h}(\mathbf{z}) = \mathbf{0} \tag{35}$$

The stability of the stationary point $\mathbf{z}^*$ is given by the linearized DAE system with respect to $\mathbf{z}^*$, which is given by

$$\mathbf{M}(\mathbf{z}^*)\frac{\partial \bar{\mathbf{z}}}{\partial t} = \mathbf{H}(\mathbf{z}^*)\bar{\mathbf{z}} \tag{36}$$

where matrix $\mathbf{H}(\mathbf{z}^*) = \frac{\partial \mathbf{h}}{\partial \mathbf{z}}(\mathbf{z}^*)$ and $\bar{\mathbf{z}}$ is a perturbation of the stationary point $\mathbf{z}^*$. The solution of Eq. (36) is addressed. Admit that there exists matrices $\mathbf{R}$ and $\mathbf{Q}$ such that

$$\mathbf{R}\mathbf{M}(\mathbf{z}^*)\mathbf{Q} = \begin{bmatrix} \mathbf{I} & \mathbf{0} \\ \mathbf{0} & \mathbf{N} \end{bmatrix} \text{ and } \mathbf{R}\mathbf{H}(\mathbf{z}^*)\mathbf{Q} = \begin{bmatrix} \mathbf{C} & \mathbf{0} \\ \mathbf{0} & \mathbf{I} \end{bmatrix} \tag{37}$$

where $\mathbf{I}$ is the identity matrix of dimension 3×3 (9×9) in the first part of Eq. (37) (in the second part of Eq. (37)), $\mathbf{C}$ is a matrix of dimension 3×3 and its main diagonal contains the 3 finite eigenvalues λ_n of the matrix pencil $(\mathbf{M}, \mathbf{H})$. Matrix $\mathbf{N}$ has dimensions 9×9 and has the property that $\mathbf{N}^k \neq 0$ for $k = 1$, but $\mathbf{N}^2 = 0$ since the DAE system has differential index one. To solve Eq. (36), write $\bar{\mathbf{z}} = \mathbf{Q}\bar{\mathbf{w}}$ and substitute into Eq. (36). Then, the resulting equation is left multiplied by $\mathbf{R}$ and taking into account Eq. (37) results in

$$\begin{bmatrix} \mathbf{I} & \mathbf{0} \\ \mathbf{0} & \mathbf{N} \end{bmatrix} \frac{d}{dt} \begin{Bmatrix} \bar{\mathbf{w}}_1 \\ \bar{\mathbf{w}}_2 \end{Bmatrix} = \begin{bmatrix} \mathbf{C} & \mathbf{0} \\ \mathbf{0} & \mathbf{I} \end{bmatrix} \begin{Bmatrix} \bar{\mathbf{w}}_1 \\ \bar{\mathbf{w}}_2 \end{Bmatrix}, \tag{38}$$

which has solution $(\bar{\mathbf{w}}_1)_n = \beta_n \exp(\lambda_n t), n = 1, \ldots, 3$ and $(\bar{\mathbf{w}}_2)_m = 0, m = 1, \ldots, 9$. λ_n are the finite eigenvalues of the matrix pencil $(\mathbf{M}, \mathbf{H})$. Therefor, if all eigenvalues λ_n has negative real part, the solution of Eq. (36) decays with time and then the stationary state $\mathbf{z}^*$ is stable. On the other hand, if at least one of the eigenvalues λ_n has positive real part, then the solution of Eq. (36) grows with time and the stationary state $\mathbf{x}^*$ is unstable. This is the stability criterion.

3.2 Basin of Attraction

To study the nonlinear stability of the single stationary point, a possibility is to construct a Lyapunov function and to check if its time derivative is non positive for a finite neighborhood of the stationary point. A candidate for the Lyapunov function is

$$V(\mathbf{p}) = \frac{1}{2}|\mathbf{p} - \mathbf{p}^*|^2 \tag{39}$$

since $V(\mathbf{p}^*) = 0$ and $V(\mathbf{p}) \geq 0$ with $\mathbf{p}^T = \{j_{l,b}\ j_{g,b}\ P_b\}$ and $\mathbf{q}$ are the other nine variables. Then

$$\dot{V}(\mathbf{p}) = \vec{\nabla} V \cdot \dot{\mathbf{p}} = \vec{\nabla} V \cdot \mathbf{F}(\mathbf{p}, \mathbf{q}(\mathbf{p})), \tag{40}$$

where $\mathbf{F}(\mathbf{p}, \mathbf{q}(\mathbf{p}))$ is obtained form Eq. (34) by writting $\dot{\mathbf{p}}$ in terms of $\dot{\mathbf{x}}$ with the help of the matrix Equation $D_{\mathbf{x}}\mathbf{g}\dot{\mathbf{x}} + D_{\mathbf{y}}\mathbf{g}\dot{\mathbf{y}} = 0$. The reduced ODE

$$\dot{\mathbf{p}} = \mathbf{F}(\mathbf{p}, \mathbf{q}(\mathbf{p})) \tag{41}$$

is more convenient than the reduced ODE given by Eq. (34) since it is easier to obtain the other nine variables in terms of the set $P_b, j_{g,b}$ and $j_{l,b}$.

Since it is possible to arbitrarily specify only three variables due to the constraints, $P_b, j_{g,b}$ and $j_{l,b}$ are chosen to vary around the domain $\mathbb{V} = \{(P_b, j_{g,b}, j_{l,b}) \in [P_t, \pi_G + P_t] \times (0, \infty) \times (0, \infty)\}$ which contains the components $P_b^*, j_{g,b}^*$ and $j_{l,b}^*$ of the stationary point. Eq. (40) is evaluated over grid points in $\bar{\mathbb{V}} \setminus (P_b^*, j_{g,b}^*, j_{l,b}^*)$, where $\bar{\mathbb{V}} = \{(P_b, j_{g,b}, j_{l,b}) \in [P_t, \pi_G + P_t] \times (0, J_{g,b}] \times (0, J_{l,B}]\}$ and $J_{g,b}$ and $J_{l,b}$ are maximum values, respectively, for the gas and liquid superficial velocities at the riser bottom. If no sign change is observed for $\dot{V}(\mathbf{p})$ and its value turn always negative, then the region $\bar{\mathbb{V}}$ forms a basin of attraction for the stationary point $\mathbf{z}^*$. The value of the other variables over $\bar{\mathbb{V}}$ are obtained by solving the constraint equation $\mathbf{g}(\mathbf{p}, \mathbf{q}) = 0$, provided that $\det D_{\mathbf{q}}\mathbf{g} \neq 0$ on the set $\bar{\mathbb{V}}$. In the process described above it is expected to obtain in $\bar{\mathbb{V}}$ a surface where $\dot{V}(\mathbf{p}) = 0$, which is part of the boundary for the basin of attraction of the stationary point $\mathbf{z}^*$. The other part of the boundary might be intersection of $\bar{\mathbb{V}} \cap \bar{\mathbb{S}}$, where $\bar{\mathbb{S}} = \{(\mathbf{p}, \mathbf{q}) \in \mathbb{L} : detD_{\mathbf{q}}\mathbf{g} = 0\}$. Notice that the analysis outlined above is restricted to the first configuration.

An interesting result to display in the system parameter and boundary conditions space would be the minimum distance of $\mathbf{z}^*(\lambda)$ to the boundary of its basin of attraction.

3.3 Poincaré Maps and Lyapunov Exponents

Poincaré maps are used to find periodic orbits and to study their stability. It could also be used to see the possibility of chaotic behavior.

To construct a Poincaré map the basic idea is to choose a hyperplane transverse to the flow generated by the DAE system. The hyperplane Σ is defined by an affine equation of the form $\mathbf{z}(t) \cdot \mathbf{n} = \alpha$, for some vector $\mathbf{n}$ and a scalar α. The Poincaré map can now be described as follows. *Let an initial condition $\mathbf{z}_0$ in the hyperplane defined by the affine equation. Then do the following.*

$i := 0, t_0 := 0$

$\mathbf{z}_0 :=$ *some initial condition for* $\mathbf{z}(t)$

repeat

starting with $t = t_i, \mathbf{z}(t_i) = \mathbf{z}_i$, *integrate* (29) *or* (30) *until* $\mathbf{z}(t) \cdot \mathbf{n} = \alpha$ *and* $\dfrac{d}{dt}(\mathbf{z}(t) \cdot \mathbf{n}) > 0$,

$\mathbf{z}_{i+1} := \mathbf{z}(t), t_{i+1} := t.$

If $||\mathbf{z}_i - \mathbf{z}_{i-1}|| < \varepsilon$ for $i > N$ with N large and ε is a given accuracy tolerance, then a periodic orbit is found with period $T = t_i - t_{i-1}$ and the Poncaré map has a fixed point $\tilde{\mathbf{z}} = \mathbf{z}_i$.

The choice of vector $\mathbf{n}$ depends on the type of stationary point, and it is chosen as the eigenvector associated with a real eigenvalue of matrix $\mathbf{H}(\mathbf{z}^*)$. Then, the value of α is chosen such that the hyperplane Σ is transverse to $\mathbf{n}$ and to the other eigenvectors (sum of the other two complex conjugate eigenvectors) associated with the other two real (complex conjugate) eigenvalues of matrix $\mathbf{H}(\mathbf{z}^*)$.

Chaotic behavior maybe characterized by divergence of orbits with close inicial conditions. Lyapunov exponents give the rate of exponential divergence with respect to a given orbit. Regions in the phase space where random behavior is apparent through the Poincaré map are candidate to have Lyapunov exponents of orbits with initial conditions in these regions evaluated.

4. RESULTS

To show results obtained from the numerical dynamics simulations, the pipeline-riser system reported in the experiments described in Vierkandt (1988) is considered. The working fluids are water and air. The separator pressure is $P_s = 10^5\ Pa$, the pipleine legth is $L_p = 9.1\ m$, the buffer equivalent length is $L_b = 10\ m$, the riser length is $L_r = 3\ m$, the pipe diameter is $D = 0.0254\ m$, the water density is $\rho_l = 998.2081\ kg/m^3$, the temperature is $T = 293.15\ K$ and the gas constant is $R_g = 287\ m^2/s^2K$ and the liquid (gas) dynamic viscosity is $\mu_l = 10^{-3}\ kg/m.s (\mu_g = 1.8 \times 10^{-5}\ kg/m.s)$. The pipeline inclination angle is $\beta = 5\pi/180\ rad$ and the riser is vertical ($\theta = pi/2\ rad$). The system parameters and the separator pressure are kept fixed, but the gas and liquid mass flow rates are allowed to vary. Therefore, the results are displayed as maps in the gas and liquid superficial velocities plane. These superficial velocities are the gas and liquid superficial velocities at the pipeline entrance.

4.1 Linear Stability Map

The first result is the linear stability map of the single stationary state, illustrated in Fig. 2 below. The vertical (horizontal) axis is the liquid (gas) superficial velocity at the pipeline entrance.

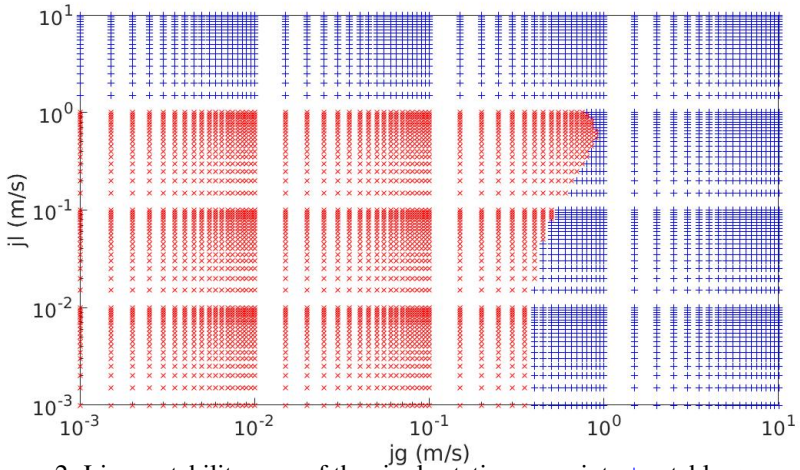

Figure 2: Linear stability map of the single stationary point. +: stable; ×: unstable

4.2 Stationary Point Local Behavior Map

More relevant information for the DAE dynamics follows in Fig. 3 below, where the single stationary point is characterized according to the real and imaginary parts of the set of three eigenvalues associated with the linearized DAE with respect to the stationary point. Figure 3 illustrate the kind of stationary point in $\mathbb{R}^3$ according to Kuznetsov (2006). The vertical (horizontal) axis is the liquid (gas) superficial velocity at the pipeline entrance. According to Fig. 3, there is the posibility of Hopf-bifurcation (stable foccus-node loses stability and becomes a unstable saddle-foccus) which agrees with experimental results, where the intermitent regime, which appears when a steady state ceases to exists, has periodic behavior.

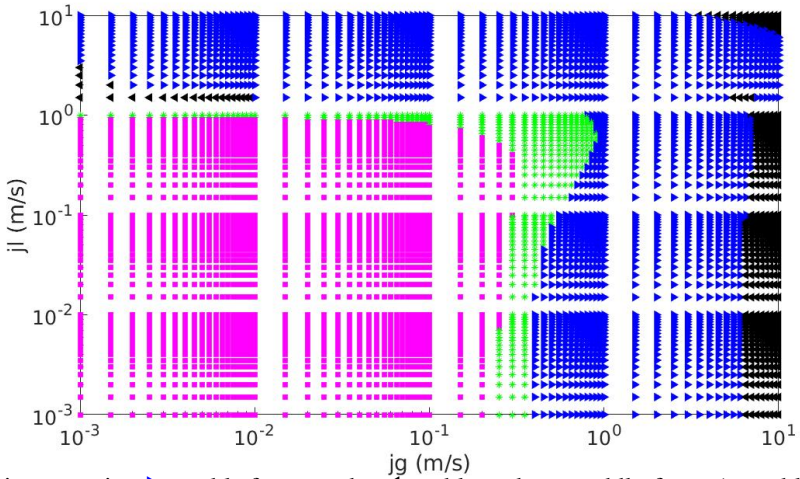

Figure 3: Type of stationary point. ▶: stable focus-node; ◀: stable node; ∗: saddle-focus (unstable focus and stabel node); ■: saddle (one eigevalue with negative part and two- eigenvalues with positive real part).

5. DISCUSSION AND CONCLUSIONS

Figure 3 above provides an idea of the bifurcation scenario as a function of the liquid and gas superficial velocities at the pipeline entrance. Hopf bifurcation happens as a focus-node loses stability and becomes a saddle-foccus. As both superficial velocities decreases, the stationary point suffers another bifurcation, from a saddle-focus to a saddle. According to experimental results, intermittent flow regime exists in the region for gas and liquid superficial velocities at the pipeline entrance where the stationary point is unstable (see Fig. 2 above). The Hopf bifurcation mentioned above leads to a periodic orbit which represents an intermittent regime, but as the stationary point suffers another bifurcation

(from saddle-focus to saddle), the trajectory topology may become more complex than just periodic orbits and chaotic behavior may arise. For gas and liquid superficial velocities values at pipeline entrance where the DAE system switches configurations, periodic orbits are expected to represent the intermittent flow regime observed in experiments.

This is a report on work in progress. As future work Poincaré maps and Lyapunov exponents will be used to find periodic orbits and to study their stability, and to study numerically the possibility of caothic behavior. The search for the stationary point basin of attraction as a function of the gas and liquid superficial velocities at the pipeline entrance, to trace the bifurcation boundaries as a function of the gas and liquid superficial velocities at the pipeline entrance and to better understand the types of bifurcation the stationary point suffers at those boundaries is also left as future work.

6. REFERENCES

Azevedo, G., Baliño, J. and Burr, K., 2015. "Linear stability analysis for severe slugging in air–water systems considering different mitigation mechanisms". *International Journal of Multiphase Flow*, Vol. 73, pp. 238–250.

Azevedo, G., Baliño, J. and Burr, K., 2017. "Influence of pipeline modeling in stability analysis for severe slugging". *Chemical Engineering Science*, Vol. 161, pp. 1–13.

Baliño, J., Burr, K. and Nemoto, R., 2010. "Modeling and simulation of severe slugging in air–water pipeline–riser systems". *International journal of multiphase flow*, Vol. 36, No. 8, pp. 643–660.

Beardmore, R. and Song, Y., 1998. "Differential-algebraic equations: A tutorial review". *International Journal of Bifurcation and Chaos*, Vol. 8, No. 07, pp. 1399–1411.

Bendiksen, K.H., 1984. "An experimental investigation of the motion of long bubbles in inclined tubes". *International journal of multiphase flow*, Vol. 10, No. 4, pp. 467–483.

Brenan, K.E., Campbell, S.L. and Petzold, L.R., 1995. *Numerical solution of initial-value problems in differential-algebraic equations*. SIAM.

Burr, K.P. and Baliño, J.L., 2015. "Evolution equation for weak hydrodynamic instabilities of two-phase flows in pipeline-riser systems".

Chen, N.H., 1979. "An explicit equation for friction factor in pipe". *Industrial & Engineering Chemistry Fundamentals*, Vol. 18, No. 3, pp. 296–297. URL `https://doi.org/10.1021/i160071a019`.

Chexal, B., Maulbetsch, J., Harrison, J., Petersen, C., Jensen, P. and Horowitz, J., 1997. "Understanding void fraction in steady state and dynamic environments".

Kuznetsov, Y.A., 2006. "Andronov-Hopf bifurcation". *Scholarpedia*, Vol. 1, No. 10, p. 1858. doi: 10.4249/scholarpedia.1858. Revision #90964.

Venkatasubramanian, V., Schattler, H. and Zaborsky, J., 1995. "Dynamics of large constrained nonlinear systems-a taxonomy theory [power system stability]". *Proceedings of the IEEE*, Vol. 83, No. 11, pp. 1530–1561.

Vierkandt, S.J., 1988. *Severe Slugging in a Pipeline-riser System: Experiments and Modeling*. Tulsa University Fluid Flow Projects.

Zakarian, E. and Tran, Q.H., 1999. "A differential-algebraic model for two-phase flow instabilities in pipeline-riser systems". *ASME-PUBLICATIONS-PVP*, Vol. 396, pp. 3–10.

7. RESPONSIBILITY NOTICE

The authors are solely responsible for the printed material included in this paper.